*Mineralogical Magazine, February 2012, Vol. 76(1), pp. 75–90*

# Carlosbarbosaite, ideally $(UO_2)_2Nb_2O_6(OH)_2 \cdot 2H_2O$, a new hydrated uranyl niobate mineral with tunnels from Jaguaraçu, Minas Gerais, Brazil: description and crystal structure

D. Atencio[1,*], A. C. Roberts[2], M. A. Cooper[3], L. A. D. Menezes Filho[4], J. M. V. Coutinho[1], J. A. R. Stirling[2], K. E. Venance[2], N. A. Ball[3], E. Moffatt[5], M. L. S. C. Chaves[4], P. R. G. Brandão[6] and A. W. Romano[4]

[1] Instituto de Geociências, Universidade de São Paulo, Rua do Lago, 562, 05508-080 São Paulo, SP, Brazil
[2] Geological Survey of Canada, 601 Booth Street, Ottawa, Ontario K1A 0E8, Canada
[3] Department of Geological Sciences, University of Manitoba, Winnipeg, Manitoba R3T 2N2, Canada
[4] Instituto de Geociências, Universidade Federal de Minas Gerais, Avenida Antônio Carlos, 6627, 31270-901 Belo Horizonte, Minas Gerais, Brazil
[5] Canadian Conservation Institute, 1030 Innes Road, Ottawa, Ontario K1A 0M5, Canada
[6] Departamento de Engenharia de Minas, Escola de Engenharia da Universidade Federal de Minas Gerais, Avenida Antônio Carlos, 6627, 31270-901 Belo Horizonte, Minas Gerais, Brazil

[*Received 31 December 2010; Accepted 1 December 2011; Associate Editor: Elena Sokolova*]

**ABSTRACT**

Carlosbarbosaite, ideally $(UO_2)_2Nb_2O_6(OH)_2 \cdot 2H_2O$, is a new mineral which occurs as a late cavity filling in albite in the Jaguaraçu pegmatite, Jaguaraçu municipality, Minas Gerais, Brazil. The name honours Carlos do Prado Barbosa (1917–2003). Carlosbarbosaite forms long flattened lath-like crystals with a very simple orthorhombic morphology. The crystals are elongated along [001] and flattened on (100); they are up to 120 μm long and 2–5 μm thick. The colour is cream to pale yellow, the streak yellowish white and the lustre vitreous. The mineral is transparent (as individual crystals) to translucent (massive). It is not fluorescent under either long-wave or short-wave ultraviolet radiation. Carlosbarbosaite is biaxial(+) with $\alpha = 1.760(5)$, $\beta = 1.775(5)$, $\gamma = 1.795(5)$, $2V_{meas.} = 70(1)^o$, $2V_{calc.} = 83^o$. The orientation is $X \parallel a$, $Y \parallel b$, $Z \parallel c$. Pleochroism is weak, in yellowish green shades, which are most intense in the $Z$ direction. Two samples were analysed. For sample 1, the composition is: $UO_3$ 54.52, CaO 2.07, $Ce_2O_3$ 0.33, $Nd_2O_3$ 0.49, $Nb_2O_5$ 14.11, $Ta_2O_5$ 15.25, $TiO_2$ 2.20, $SiO_2$ 2.14, $Fe_2O_3$ 1.08, $Al_2O_3$ 0.73, $H_2O$ (calc.) 11.49, total 104.41 wt.%; the empirical formula is $(\square_{0.68}Ca_{0.28}Nd_{0.02}Ce_{0.02})_{\Sigma=1.00}[U_{1.44}\square_{0.56}O_{2.88}(H_2O)_{1.12}](Nb_{0.80}Ta_{0.52}Si_{0.27}Ti_{0.21}Al_{0.11}Fe_{0.10})_{\Sigma=2.01}O_{4.72}(OH)_{3.20}(H_2O)_{2.08}$. For sample 2, the composition is: $UO_3$ 41.83, CaO 2.10, $Ce_2O_3$ 0.31, $Nd_2O_3$ 1.12, $Nb_2O_5$ 14.64, $Ta_2O_5$ 16.34, $TiO_2$ 0.95, $SiO_2$ 3.55, $Fe_2O_3$ 0.89, $Al_2O_3$ 0.71, $H_2O$ (calc.) 14.99, total 97.43 wt.%; the empirical formula is $(\square_{0.67}Ca_{0.27}Nd_{0.05}Ce_{0.01})_{\Sigma=1.00}[U_{1.04}\square_{0.96}O_{2.08}(H_2O)_{1.92}](Nb_{0.79}Ta_{0.53}Si_{0.42}Ti_{0.08}Al_{0.10}Fe_{0.08})_{\Sigma=2.00}O_{4.00}(OH)_{3.96}(H_2O)_{2.04}$. The ideal endmember formula is $(UO_2)_2Nb_2O_6(OH)_2 \cdot 2H_2O$. Calculated densities are 4.713 g cm$^{-3}$ (sample 1) and 4.172 g cm$^{-3}$ (sample 2). Infrared spectra show that both (OH) and $H_2O$ are present. The strongest eight X-ray powder-diffraction lines [listed as $d$ in Å($I$)($hkl$)] are: 8.405(8)(110), 7.081(10)(200), 4.201(9)(220), 3.333(6)(202), 3.053(8)(022), 2.931(7)(420), 2.803(6)(222) and 2.589(5)(040,402). The crystal structure was solved using single-crystal X-ray diffraction ($R = 0.037$) which gave the following data: orthorhombic, *Cmcm*, $a = 14.150(6)$, $b = 10.395(4)$, $c = 7.529(3)$ Å, $V = 1107(1)$ Å$^3$, $Z = 4$. The

* E-mail: datencio@usp.br
DOI: 10.1180/minmag.2012.076.1.75

crystal structure contains a single *U* site with an appreciable deficiency in electron scattering, which is populated by U atoms and vacancies. The *U* site is surrounded by seven O atoms in a pentagonal bipyramidal arrangement. The *Nb* site is coordinated by four O atoms and two OH groups in an octahedral arrangement. The half-occupied tunnel *Ca* site is coordinated by four O atoms and four $H_2O$ groups. Octahedrally coordinated Nb polyhedra share edges and corners to form $Nb_2O_6(OH)_2$ double chains, and edge-sharing pentagonal bipyramidal U polyhedra form $UO_5$ chains. The $Nb_2O_6(OH)_2$ and $UO_5$ chains share edges to form an open U−Nb−φ framework with tunnels along [001] that contain $Ca(H_2O)_4$ clusters. Carlosbarbosaite is closely related to a family of synthetic U−Nb−O framework tunnel structures, it differs in that is has an (OH)-bearing framework and $Ca(H_2O)_4$ tunnel occupant. The structure of carlosbarbosaite resembles that of holfertite.

**Keywords:** carlosbarbosaite, Jaguaraçu, Minas Gerais, Brazil, uranium minerals, niobium minerals, mineral structures, holfertite, U−Nb−O frameworks.

## Introduction

CARLOSBARBOSAITE, ideally $(UO_2)_2Nb_2O_6(OH)_2{\cdot}2H_2O$, from the Jaguaraçu pegmatite, Jaguaraçu municipality, Minas Gerais, Brazil, has been approved by the CNMNC (IMA 2010-047) as a new mineral species. The name honours Carlos do Prado Barbosa (1917−2003) who graduated as a chemical engineer in 1943. Carlos had a long career as a dealer in mineral specimens, and paid special attention to the discovery and study of rare mineral species, especially from the Brumado magnesite mine, Bahia, Brazil, and the pegmatites of Minas Gerais, including the Jaguaraçu pegmatite. He was a co-author of the descriptions of bahianite (Moore *et al.* 1978) and minasgeraisite-(Y) (Foord *et al.* 1986).

The structure of carlosbarbosaite resembles that of holfertite (Sokolova *et al*., 2005; Belakovskiy *et al*., 2006), but it is reasonably well ordered whereas holfertite is disordered. Holfertite is 04.GB.70 in the Nickel-Strunz classification. Carlosbarbosaite is probably identical to the "U-Nb-oxide" described from Argentina by Arcidiácono and Bedlivy (1976) which is UM 1976-11-O:NbU in Smith and Nickel (2007). The X-ray powder diffraction pattern is similar to ICDD 00-29-1373 (the unnamed Argentinian mineral) and the optical data are also similar. It may also be known from the Eastern Desert of Egypt (Abd El-Naby, 2008). Type material is deposited in the collections of the Museu de Geociências, Instituto de Geociências, Universidade de São Paulo, Rua do Lago, 562, 05508-080 São Paulo, Brazil, registration number DR707. Microgram portions are housed in the Systematic Reference Series of the National Mineral Collection at the Geological Survey of Canada, 601 Booth Street, Ottawa, Ontario K1A 0E8, Canada.

## Occurrence

Carlosbarbosaite was found in the Jaguaraçu pegmatite, Jaguaraçu municipality (19º38′57″S 42º44′59″W), Minas Gerais, Brazil. The pegmatite body, also known as the Lavra do Sr José Pinto, is located adjacent to a football pitch. It is lenticular, with a strike length of at least 100 m and a maximum width of 20 m, and crops out on a steep hillside; at its uppermost end it pinches to less than 1 m in width.

Quartz, orthoclase (also var. adularia), microcline (var. amazonite), albite, muscovite, beryl, elbaite, schorl, spodumene, fluorapatite, fluorite, almandine−spessartine, lepidolite and biotite series minerals, anatase, cassiterite, uraninite, pyrite, zircon, columbite-(Fe), tapiolite-(Fe), cerussite, pyromorphite, monazite-(Ce), euxenite-(Y), chernovite-(Y), milarite, minasgeraisite-(Y), churchite-(Y), hematite, ilmenite, magnetite, manganese oxides, kaolinite, montmorillonite and nontronite have been identified from the pegmatite (Foord *et al*., 1986; Cassedanne and Alves 1994). It is the type locality for minasgeraisite-(Y) (Foord *et al*., 1986).

Carlosbarbosaite occurs as a late-stage cavity filling in albite, it is closely associated with zircon, muscovite, kaolinite and columbite-(Fe).

## Habit and physical properties

Carlosbarbosaite occurs as long flattened lath-like crystals with a simple orthorhombic morphology. The observed forms are the pinacoids {001}, {010} and {100}. Twinning was not observed. The crystals are elongated along [001] and

flattened on (100). The fibres have a rectangular cross section and are bounded by (100) and (010); these also appear to be cleavage planes (Figs 1 and 2). The crystals are up to 120 μm long and 2−5 μm thick. Larger crystals commonly have aspect ratios in excess of 10:1. Some material is fibrous and powdery. The vast majority of the elongated fibres are bent.

Carlosbarbosaite is cream to pale yellow, the streak is yellowish white and the lustre vitreous. The mineral is transparent (as individual crystals) to translucent (in massive form). It is not fluorescent in either long-wave or short-wave ultraviolet radiation. The Mohs hardness was not determined as too little pure material was available, but the mineral is easily crushed

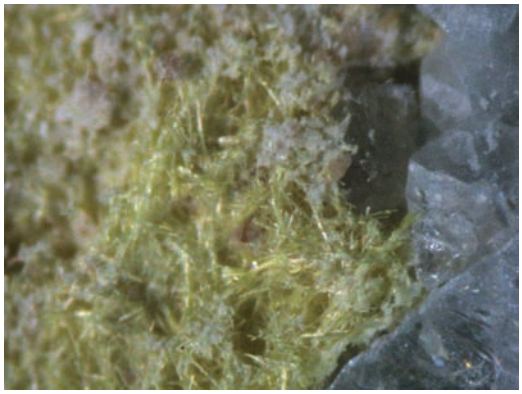

FIG. 1. Carlosbarbosaite from Jaguaraçu, Minas Gerais, Brazil. The field of view is ~3 mm across.


FIG. 2. Back-scattered electron images of carlosbarbosaite.

between two glass slides; its tenacity is flexible. The cleavage forms are presumed to be {100} and {010}; parting was not observed and the fracture is uneven. The density could not be measured because too little pure material was available; the calculated density based on the empirical formula and unit-cell parameters derived from the single-crystal structure study is 4.713 g $cm^{-3}$ (sample 1), 4.172 g $cm^{-3}$ (sample 2) [see below].

In transmitted light, carlosbarbosaite is biaxial (+) with $\alpha$ = 1.760(5), $\beta$ = 1.775(5), $\gamma$ = 1.795(5), $2V_{meas.}$ = 70(1)º, $2V_{calc.}$ = 82.6º (white light). The orientation is $X \parallel a$, $Y \parallel b$, $Z \parallel c$. Pleochroism is weak, in yellowish green shades, which are most intense in the $Z$ direction.

The infrared (IR) spectrum (Fig. 3) indicates that both (OH) and $H_2O$ are present in the structure. A strong band at 3376 $cm^{-1}$ is due to O–H stretching in both (OH) and $H_2O$; a peak at 1638 $cm^{-1}$ is due to H–O–H bending in $H_2O$ molecules. The bands at 878 and 621 $cm^{-1}$ are due to $NbO_6$ vibrations. The band at 878 $cm^{-1}$ is due to the uranyl ion. There are no bands in the spectra that are indicative of carbonate ions.

## Chemical data

Several crystals of carlosbarbosaite were analysed in Brazil (sample 1) and in Canada (sample 2). Mean analytical results are given in Table 1.

### *Sample 1*

Seven point analyses of seven different crystals were carried out on a Stereoscan S440 scanning electron microscope (SEM) fitted with an INCA microanalysis system with energy-dispersive spectrometry (EDS) and wavelength-dispersive spectrometry (WDS), at the Departamento de Engenharia de Minas e Petróleo da Universidade de São Paulo. The elements Si and Ti were analysed by WDS, and the other elements by EDS. Operating conditions were 15 kV, 10 nA, with an ~5 μm beam diameter and a count time of 20 s. The use of a SEM with both EDS and WDS systems allows quantitative analysis of materials that are too fine grained or beam sensitive for analysis using an electron microprobe. The $H_2O$ content was calculated by stoichiometry on the basis of the crystal-structure analysis; the presence of $H_2O$ was confirmed by IR spectroscopy. Not enough pure material was available for water determination by classical methods.

### *Sample 2*

Seven chemical analyses were carried out on a Cameca SX50 electron microprobe at the Geological Survey of Canada, Ottawa, Ontario in WDS mode. Operating conditions were an accelerating potential of 20 kV, a probe current of 5 nA, a 1–2 μm beam diameter and counting times of 10 s on the peak and 5 s on the background.

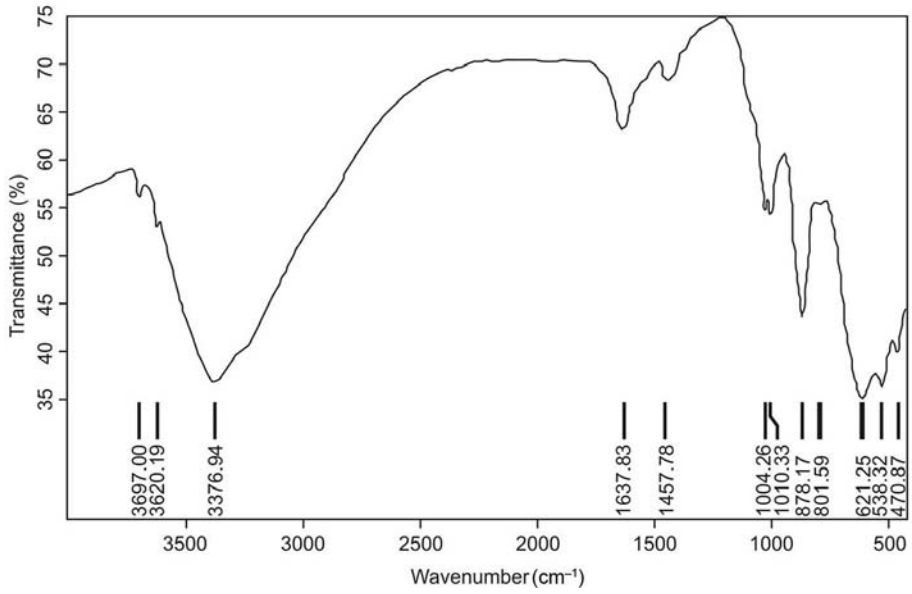


FIG. 3. The infrared spectrum of carlosbarbosaite.

TABLE 1. Chemical data for carlosbarbosaite.

| Constituent | — WDS/EDS Sample 1 — Mean (wt.%) | Range (wt.%) | Standard | ——— WDS Sample 2 ——— Mean (wt.%) | Range (wt.%) | Standard |
|---|---|---|---|---|---|---|
| $UO_3$ | 54.52 | 53.22–55.94 | $UO_2$ | 41.83 | 39.81–43.39 | $UO_2$ |
| CaO | 2.07 | 1.98–2.15 | calcite | 2.10 | 1.99–2.23 | wollastonite |
| $Ce_2O_3$ | 0.33 | 0.25–0.41 | $CeAl_2$ | 0.31 | 0.00–0.87 | $CePO_4$ |
| $Nd_2O_3$ | 0.49 | 0.26–0.74 | $NdF_3$ | 1.12 | 0.84–1.54 | $NdPO_4$ |
| $Nb_2O_5$ | 14.11 | 13.74–14.46 | Nb | 14.64 | 14.25–15.00 | Nb |
| $Ta_2O_5$ | 15.25 | 14.41–16.16 | Ta | 16.34 | 14.87–17.54 | Ta |
| $TiO_2$ | 2.20 | 2.03–2.32 | Ti | 0.95 | 0.20–1.38 | Ti |
| $SiO_2$ | 2.14 | 2.02–2.22 | $SiO_2$ | 3.55 | 3.24–3.79 | $SiO_2$ |
| $Fe_2O_3$ | 1.08 | 1.04–1.10 | Fe | 0.89 | 0.71–1.06 | FeO |
| $Al_2O_3$ | 0.73 | 0.68–0.83 | Al | 0.71 | 0.65–0.76 | $Al_2O_3$ |
| $H_2O$* | 11.49 | | | 14.99 | | |
| Total | 104.41 | | | 97.43 | | |

* The $H_2O$ content is calculated on the basis of the assigned O:(OH):($H_2O$) ratio (see text).

The uranium content was found to vary significantly from crystal to crystal. The narrow fibre morphology and high water content made quantitative analysis difficult. Here we present two sets of reliable chemical data that cover the range in observed $UO_3$ content. The crystal-structure analysis revealed a single *U* site with an appreciable deficiency in electron scattering, populated by uranium atoms and vacancies. If the *U* site is occupied by $U^{6+}$, the resulting anion in the formula unit is $O_{10}(OH)_2(H_2O)_2$, if the U-site is occupied by a vacancy, the anion is $O_2(OH)_6(H_2O)_6$. The chemical data (samples 1 and 2) are normalized to fourteen anions, with the O:(OH):($H_2O$) ratio adjusted in response to both the U content and octahedral cation ($Nb^{5+}$ + $Ta^{5+}$ + $Si^{4+}$ + $Ti^{4+}$ + $Al^{3+}$ + $Fe^{3+}$) sum. The anion O:(OH):($H_2O$) ratio is a simple combination of the U-bearing anion composition $[O_{10}(OH)_2(H_2O)_2]_x$ and the □-bearing anion composition $[O_2(OH)_6(H_2O)_6]_{(1-x)}$. For normalization of the sample 1 chemical data $x = 0.70$, for the sample 2 data $x = 0.51$. Empirical formulae (based on 14 anions) are as follows: $(\square_{0.68}Ca_{0.28}Nd_{0.02}Ce_{0.02})_{\Sigma=1.00}[U_{1.44}\square_{0.56}O_{2.88}(H_2O)_{1.12}](Nb_{0.80}Ta_{0.52}Si_{0.27}Ti_{0.21}Al_{0.11}Fe_{0.10})_{\Sigma=2.01}O_{4.72}(OH)_{3.20}(H_2O)_{2.08}$ for sample 1 and $(\square_{0.67}Ca_{0.27}Nd_{0.05}Ce_{0.01})_{\Sigma=1.00}[U_{1.04}\square_{0.96}O_{2.08}(H_2O)_{1.92}](Nb_{0.79}Ta_{0.53}Si_{0.42}Ti_{0.08}Al_{0.10}Fe_{0.08})_{\Sigma=2.00}O_{4.00}(OH)_{3.96}(H_2O)_{2.04}$ for sample 2.

For each composition, the *Ca* site is dominated by a vacancy, the *U* site by $U^{6+}$ and the *Nb* site by $Nb^{5+}$. The chemical variation at the *U* site and the anion sites is greater than the variation at the tunnel *Ca* and octahedral *Nb* sites. Simplified chemical compositions are expressed in terms of the U-bearing and □-bearing endmembers in Table 2.

Despite the absence of tetrahedral sites suitable for Si in the carlosbarbosaite structure, octahedral

TABLE 2. Carlosbarbosaite compositions in terms of the hypothetical endmembers.

| | U-bearing endmember $(UO_2)_2Nb_2O_6(OH)_2(H_2O)_2$ | □-bearing endmember $(H_2O)_4Nb_2[O_2(OH)_4](OH)_2(H_2O)_2$ |
|---|---|---|
| Sample 1 | 0.70 | 0.30 |
| Sample 2 | 0.51 | 0.49 |
| Sample 1 | $(UO_2)_{1.40}(\square(H_2O)_2)_{0.60}Nb_2[O_{4.80}(OH)_{1.20}](OH)_2(H_2O)_2$ | |
| Sample 2 | $(UO_2)_{1.02}(\square(H_2O)_2)_{0.98}Nb_2[O_{4.04}(OH)_{1.96}](OH)_2(H_2O)_2$ | |

TABLE 3. X-ray powder diffraction data for carlosbarbosaite.

| | $I$ (%) | $d_{meas.}$ (Å) | $d_{calc.}$ (Å) | $h$ | $k$ | $l$ |
|---|---|---|---|---|---|---|
| | **80** | **8.405** | 8.388 | 1 | 1 | 0 |
| | **100** | **7.081** | 7.089 | 2 | 0 | 0 |
| | 5 | 5.591 | 5.613 | 1 | 1 | 1 |
| * | 15 | 5.208 | 5.203 | 0 | 2 | 0 |
| * | 20 | 4.306 | 4.303 | 3 | 1 | 0 |
| * | **90** | **4.201** | 4.194 | 2 | 2 | 0 |
| * | 20 | 3.762 | 3.776 | 0 | 0 | 2 |
| * | 10 | 3.659 | 3.667 | 2 | 2 | 1 |
| * | 5 | 3.541 | 3.544 | 4 | 0 | 0 |
| * | 30 | 3.443 | 3.443 | 1 | 1 | 2 |
| * | **60** | **3.333** | 3.333 | 2 | 0 | 2 |
| * | **80** | **3.053** | 3.056 | 0 | 2 | 2 |
| * | **70** | **2.931** | 2.929 | 4 | 2 | 0 |
| * | **60** | **2.803** | 2.806 | 2 | 2 | 2 |
| * | 10 | 2.736 | 2.736 | 5 | 1 | 0 |
| | | | 2.601 | 0 | 4 | 0 |
| | **50** | **2.589** | 2.584 | 4 | 0 | 2 |
| * | 10 | 2.512 | 2.514 | 1 | 3 | 2 |
| * | 20 | 2.445 | 2.442 | 2 | 4 | 0 |
| | 3 | 2.406 | 2.411 | 1 | 1 | 3 |
| * | 5 | 2.363 | 2.363 | 6 | 0 | 0 |
| | | | 2.324 | 2 | 4 | 1 |
| | 20 | 2.319 | 2.314 | 4 | 2 | 2 |
| * | 10 | 2.265 | 2.266 | 0 | 2 | 3 |
| * | 20 | 2.195 | 2.195 | 5 | 3 | 0 |
| | | | 2.158 | 2 | 2 | 3 |
| | 15b | 2.151 | 2.151 | 6 | 2 | 0 |
| * | 20 | 2.109 | 2.108 | 5 | 3 | 1 |
| * | 30 | 2.049 | 2.051 | 2 | 4 | 2 |
| * | 10 | 2.022 | 2.021 | 4 | 4 | 1 |
| | 3 | 2.003 | 2.003 | 6 | 0 | 2 |
| * | 10 | 1.923 | 1.923 | 7 | 1 | 1 |
| * | 25 | 1.890 | 1.888 | 0 | 0 | 4 |
| * | 15 | 1.869 | 1.869 | 6 | 2 | 2 |
| * | 50 | 1.833 | 1.833 | 4 | 4 | 2 |
| | | | 1.809 | 0 | 4 | 3 |
| | 3 | 1.805 | 1.808 | 1 | 5 | 2 |
| * | 10 | 1.772 | 1.772 | 8 | 0 | 0 |
| | | | 1.753 | 2 | 4 | 3 |
| | 20 | 1.749 | 1.749 | 6 | 4 | 0 |
| * | 25 | 1.722 | 1.722 | 2 | 2 | 4 |
| | | | 1.704 | 6 | 4 | 1 |
| | 3 | 1.705 | 1.704 | 7 | 3 | 1 |
| | | | 1.690 | 0 | 6 | 1 |
| | 3 | 1.687 | 1.685 | 2 | 6 | 0 |
| * | 15b | 1.644 | 1.644 | 2 | 6 | 1 |
| * | 10 | 1.611 | 1.611 | 4 | 4 | 3 |
| * | 40 | 1.586 | 1.587 | 4 | 2 | 4 |
| | | | 1.560 | 7 | 1 | 3 |
| | 20 | 1.558 | 1.558 | 4 | 6 | 0 |
| | | | 1.533 | 8 | 2 | 2 |
| | 35b | 1.531 | 1.528 | 0 | 4 | 4 |
| | | | 1.525 | 9 | 1 | 1 |

Si is possible; $Si(OH)_6^{2-}$ is stable at low pressure and temperature in thaumasite, $Ca_3[Si(OH)_6][SO_4][CO_3]\cdot 12H_2O$ (Edge and Taylor, 1971). The real restriction on the occurrence of $^{[6]}Si$ in crystal structures is the crowding of cations around oxygen ions (O'Keeffe and Hyde, 1981). The occurrence of $^{[6]}Si$ in pyrochlore-group minerals was discussed by Atencio *et al.* (2010). Carlosbarbosaite might be an example of a mineral with mixed occupancies of a key domain. Unlike sites *sensu stricto*, domains can be defined as micro-regions in the unit cell that can host a number of alternative sites having, in a general case, different coordination numbers, as in eudialyte-group minerals (Nomura *et al*., 2010). If this hypothesis were correct, $NbO_6$ octahedra would be 'replaced' by $SiO_4$ tetrahedra. If Nb was present in the micro-region, the coordination number would be 6, and if Si was present, it would be 4. We have, however, no evidence to support this hypothesis.

The formulae for samples 1 and 2 contain more of the U-bearing endmember ($x$ >0.5) and we therefore designate $(UO_2)_2Nb_2O_6(OH)_2(H_2O)_2$ as the endmember composition. Minor Ca + *REE* occupy the channel *Ca* site, and minor tetravalent cations (Si and Ti) and trivalent cations (Fe and Al) are present at the octahedrally coordinated *Nb* site (Table 7). The Nb/(Nb + Ta) ratio is constant at ~0.6.

## Crystallography

X-ray powder-diffraction data obtained using a 114.6 mm diameter Debye-Scherrer powder camera with Ni-filtered Cu$K\alpha$ radiation ($\lambda$ = 1.5418 Å) are listed in Table 3. These data are not corrected for film shrinkage and no internal standard was used. The unit-cell parameters refined from the powder data are $a$ = 14.177(3), $b$ = 10.405(3), $c$ = 7.552(2) Å, $V$ = 1114.0(5) Å$^3$, $Z$ = 4; they are in close agreement with those obtained from the single-crystal study. The $a$:$b$:$c$ axial ratio calculated from the unit-cell parameters is 1.363:1:0.726.

Calculations using the Gladstone–Dale relationship based on the empirical formulae and the unit-cell data derived from single-crystal studies

* Lines used in the determination of the unit-cell parameters.

yield values for $1 - (K_p/K_c)$ of 0.124 for sample 1 (indicating poor compatibility) and 0.059 for sample 2 (indicating good compatibility) (Mandarino, 1979). According to Mandarino (1989), 27% of the oxides are in the lower two categories of fair or poor compatibility. This is in accord with the earlier conclusion of Mandarino (1981) that the Gladstone–Dale relationship is not applicable to all oxide minerals.

## Single-crystal X-ray study

A single crystal ($2 \times 7 \times 50$ μm) of carlosbarbosaite was mounted on a Bruker D8 three-circle diffractometer equipped with a rotating anode generator (Mo$K\alpha$ radiation), multi-layer optics and an APEX-II CCD detector. The intensities of 9510 reflections were collected to 46º2θ using 60 s per 0.3º frame and a crystal-to-detector distance of 5 cm. Empirical absorption corrections (*SADABS*; Sheldrick, 1998) were applied and identical data merged to give 3026 reflections covering the entire Ewald sphere. Unit-cell parameters were obtained by least-squares refinement of 2929 reflections [$I > 8\sigma(I)$], and are given in Table 4 along with other pertinent crystallographic details.

The crystal structure was solved by direct methods and refined in space group *Cmcm* with the Bruker *SHELXTL* Version 5.1 system of programs (Sheldrick, 1997) to a final $R_1$ index of 3.7% using a fully anisotropic model. Precession slices constructed from the single crystal diffraction data reveal that the crystal investigated is not an ideal simple single crystal, and contains several minor domains offset marginally from the principal crystal. Fractional atom coordinates and anisotropic displacement parameters are given in Table 5; selected bond distances in Table 6; refined site-scattering values in Table 7 and bond valences in Table 8. The *U* site is surrounded by seven O atoms in a pentagonal bipyramidal arrangement. The presence of the uranyl ion $(UO_2)^{2+}$, with U–O bond lengths of ~1.8 Å (Table 6), indicates that the U in the structure is present as $U^{6+}$; this result is in accord with the bond-valence sum for the *U* site (Table 8). The *Nb* site is coordinated by four O atoms and two OH groups in an octahedral arrangement with a $\langle Nb-\varphi \rangle$ distance (where φ denotes an unspecified anion) of 1.974 Å. The *Ca* site is coordinated by four uranyl O atoms and four $H_2O$ groups, with a $\langle Ca-\varphi \rangle$ distance of 2.463 Å (Table 5). Chemical analysis of the sample used for crystal structure refinement was not carried out in order to preserve it; the chemical data in Table 1 were used as a guide in the interpretation the structure refinement result. The three cation sites in carlosbarbosaite (*U*, *Nb*, *Ca*) reside at the (8*g*, 8*e*, 4*c*) sites, respectively, and contribute (2, 2, 1) a.p.f.u. (atoms per formula unit) each. Simple inspection of the chemical constituents in Table 4 reveals that all three cation sites within the structure are occupied by two or more chemical constituents with significantly different X-ray scattering values. As such, the structure refinement needs to be carried out with site-occupancy refinement of all three cation sites simultaneously. As expected, the refining site occupancies show extreme correlation with the overall scale factor, leading to greater uncertainties in the refined occupancy values. Two refinement models were tested: model A, using neutral cation and oxygen scattering factors, and model B, using neutral cation scattering factors and an ionic scattering factor for oxygen. Models A and B gave total refined scattering values for the three cation sites of 234(11) and 254(12) electrons, respectively, in comparison with 223 and 187 electrons given by the two sets of chemical data (Tables 1 and 7). We

TABLE 4. Miscellaneous crystallographic information for carlosbarbosaite.

| | | | |
|---|---|---|---|
| *a* (Å) | 14.150(6) | Crystal size (μm) | $2 \times 7 \times 50$ |
| *b* (Å) | 10.395(4) | Radiation | Mo$K\alpha$ |
| *c* (Å) | 7.529(3) | No. of reflections | 9510 |
| *V* (Å$^3$) | 1107.4(1.3) | No. in Ewald sphere | 3026 |
| Space group | *Cmcm* | No. with $Fo > 4\sigma(F)$ | 455 |
| *Z* | 4 | $R_{merge}$% | 7.6 |
| | | $R_1$% | 3.7 |
| | | *wR*2% | 9.4 |

TABLE 5. Fractional atom coordinates and anisotropic displacement parameters (Å$^2$) for carlosbarbosaite.

| Site | *x/a* | *y/b* | *z/c* | $U_{11}$ | $U_{22}$ | $U_{33}$ | $U_{23}$ | $U_{13}$ | $U_{12}$ | $U_{eq}$ |
|---|---|---|---|---|---|---|---|---|---|---|
| *U* | 0.26634(7) | 0.27203(10) | ¼ | 0.0279(6) | 0.0507(7) | 0.0244(6) | 0 | 0 | −0.0115(5) | 0.0343(4) |
| *Nb* | 0.38296(12) | ½ | 0 | 0.0133(10) | 0.0443(14) | 0.0267(12) | −0.0001(8) | 0 | 0 | 0.0281(8) |
| *Ca* | ½ | 0.0127(17) | ¼ | 0.055(13) | 0.051(13) | 0.066(14) | 0 | 0 | 0 | 0.057(8) |
| O(1) | 0.3622(14) | 0.1709(16) | ¼ | 0.097(16) | 0.062(13) | 0.023(8) | 0 | 0 | −0.047(11) | 0.061(6) |
| O(2) | 0.1633(12) | 0.3780(15) | ¼ | 0.048(11) | 0.058(11) | 0.035(9) | 0 | 0 | −0.000(9) | 0.047(5) |
| O(3) | 0.3020(7) | 0.3571(10) | −0.0398(13) | 0.026(6) | 0.052(7) | 0.027(5) | 0.008(5) | −0.003(5) | −0.015(5) | 0.035(3) |
| O(4) | 0.3758(9) | 0.4471(14) | ¼ | 0.022(8) | 0.042(9) | 0.015(7) | 0 | 0 | −0.001(6) | 0.026(4) |
| OH | ½ | 0.6106(14) | 0.0547(17) | 0.027(8) | 0.051(10) | 0.022(7) | 0.003(7) | 0 | 0 | 0.033(4) |
| OW | ½ | 0.126(3) | −0.022(3) | 0.12(3) | 0.10(2) | 0.075(19) | −0.001(15) | 0 | 0 | 0.096(14) |

used model B for comparison with the chemistry in Table 1, as the site scattering at the octahedrally coordinated *Nb* site appears to be in better agreement with the observed chemistry. The crystal selected for single XRD analysis appears to contain slightly more U than either of the chemical analyses suggest (i.e. model A: $148e^- = U_{1.61}$; model B: $160e^- = U_{1.74}$). The species that is most closely related to carlosbarbosaite is the recently described mineral holfertite, in which a structure is reported with *U* sites containing $U^{6+}_{1.75}\ \square_{0.25}$, and 1.74 $U^{6+}$ from electron microprobe analysis (Sokolova *et al*., 2005; Belakovskiy *et al*., 2006). Both holfertite and carlosbarbosaite show a similar deficiency in $U^{6+}$ (relative to an ideal sum of 2).

## Description of the structure

### *The $(UO_2)_2Nb_2O_6(OH)_2(H_2O)_2$ endmember*

In carlosbarbosaite, pairs of $NbO_4(OH)_2$ octahedra share their OH−OH edge to form $Nb_2O_8(OH)_2$ dimers that link along [001] to other dimers at their O-vertices, to form a $Nb_2O_6(OH)_2$ double chain (Fig. 4*a*). Pentagonal bipyramids of U polyhedra link along their O(3)−O(3) edges to form $UO_5$ chains parallel to [001] (Fig. 4*b*), and the $UO_5$ and $Nb_2O_6(OH)_2$ chains share O(3)−O(4) edges to form an open U−Nb−φ framework with tunnels along [001] that contain $Ca(H_2O)_4$ clusters (Fig. 5). In carlosbarbosaite, each $Nb_2O_6(OH)_2$ double chain links to four $UO_5$ chains, and each $UO_5$ chain, in turn, links to two $Nb_2O_6(OH)_2$ double chains forming square-shaped tunnels. In the related mineral holfertite, chains of edge-sharing U polyhedra (six coordinate) share vertices with single chains of $Ti_5$ bipyramids to form similar tunnels that also contain $Ca(H_2O)_x$ clusters; each Ti−φ chain links to three flanking $UO_4$ chains, and each $UO_4$ chain, in turn, links to two Ti−φ chains to form triangular-shaped tunnels (Sokolova *et al*., 2005). The triangular-shaped tunnels in holfertite are wider and the Ca−$H_2O$ tunnel occupants show appreciable positional disorder, in comparison to the more compact square-shaped tunnels in carlosbarbosaite which contain reasonably well ordered $Ca(H_2O)_4$ clusters. A cut-away view along the tunnel in carlosbarbosaite is shown in Fig. 6; portions of the two $Nb_2O_6(OH)_2$ double chains that border the tunnel are at the margins, and a 50% alternating occupation of the *Ca* site is shown within the tunnel. The *Ca* site forms four weak

TABLE 6. Selected interatomic distances and angles for carlosbarbosaite.

| | | | |
|---|---|---|---|
| *U*–O(1) | 1.72(2) | *Ca*–O(1) | 2.55(2) ×2 |
| *U*–O(2) | 1.827(16) | *Ca*–O(2) | 2.702(18) ×2 |
| *U*–O(3) | 2.289(10) ×2 | *Ca*–OW | 2.24(3) ×2 |
| *U*–O(3) | 2.408(10) ×2 | *Ca*–OW | 2.36(3) ×2 |
| *U*–O(4) | 2.390(13) | ⟨***Ca*–φ**⟩ | **2.463** |
| ⟨***U*–O$_{ur}$**⟩ | **1.774** | | |
| ⟨***U*–O$_{eq}$**⟩ | **2.357** | | |
| *Nb*–O(3) | 1.900(10) ×2 | OH···OW | 2.75(4) |
| *Nb*–O(4) | 1.964(4) ×2 | OW···O(2) | 2.877(19) ×2 |
| *Nb*–OH | 2.057(9) ×2 | O(2)–OW–O(2) | 106.9(9) |
| ⟨***Nb*–φ**⟩ | **1.974** | | |

Mean values are listed in bold.

bonds to uranyl oxygen ions (Table 8), and four stronger bonds to the $H_2O$ groups that lie above and below the Ca position. The H-bond from the OH group is directed towards the $H_2O$ group, and each $H_2O$ group directs H-bonds towards the uranyl O(2) position (Fig. 6; Table 8).

### *The $(H_2O)_4Nb_2[O_2(OH)_4](OH)_2(H_2O)_2$ endmember*

If the *U* site is occupied by vacancy, local bond-valence arguments suggest the following changes to the anion: O(1) and O(2) sites are occupied by $H_2O$ groups and the O(3) site is occupied by an (OH) group (Table 8). The O(4) site remains occupied by $O^{2-}$, receiving additional H-bonding as required. The *Nb* site is coordinated by 2 $O^{2-}$ + 4 (OH) anions, and the *Ca* site by 8 $H_2O$ groups. The complete anion chemistry (p.f.u.) for the □-bearing endmember on a site basis is: O(1) = $(H_2O)_2$, O(2) = $(H_2O)_2$, O(3) = $(OH)_4$, O(4) = $O_2^{2-}$, OH = $(OH)_2$ and OW = $(H_2O)_2$; this gives $O_2(OH)_6(H_2O)_6$ for the fourteen anions.

## Related U–Nb–O tunnel compounds

A very similar tunnel structure is observed in the compound $Cs(UO_2)_2Nb_2(O_{7.5}\square_{0.5})$, which also

TABLE 7. Refined site-scattering values (e.p.f.u.)* for carlosbarbosaite.

| Site | Structure refinement | | Electron microprobe | | |
|---|---|---|---|---|---|
| | Electrons<br>$O_{neutral}$<br>$O_{ionic}$ | < *r* >** | Assignment (Sample 1) a.p.f.u.<br>Assignment (Sample 2) a.p.f.u. | Electrons | < *r* > |
| *U* | 148(3) | 0.83 | $U_{1.44}\square_{0.56}$ | 132 | 0.81 |
| | 160(4) | | $U_{1.04}\square_{0.96}$ | 96 | 0.81 |
| *Nb* | 78(2) | 0.61 | $Nb_{0.80}Ta_{0.52}Si_{0.27}Ti_{0.21}Al_{0.11}Fe_{0.10}$ | 83 | 0.60 |
| | 85(2) | | $Nb_{0.79}Ta_{0.53}Si_{0.42}Ti_{0.08}Al_{0.10}Fe_{0.08}$ | 82 | 0.58 |
| *Ca* | 7.8(6) | 1.11 | $\square_{0.68}Ca_{0.28}Nd_{0.02}Ce_{0.02}$ | 8 | 1.12 |
| | 8.6(6) | | $\square_{0.67}Ca_{0.27}Nd_{0.05}Ce_{0.01}$ | 9 | 1.12 |
| | 234 | | (Total electrons) | 223 | |
| | 254 | | | 187 | |

* The abbreviation e.p.f.u. is electrons per formula unit.
** The (observed mean bond length − calculated mean anion radius).

TABLE 8. Bond-valence analysis for carlosbarbosaite.*

| | *U* | *Nb* | *Ca* | Sum | [H(1)] | [H(2)] | [H(3)] | Sum |
|---|---|---|---|---|---|---|---|---|
| O(1) | 1.89 | | $0.21^{\times 2}\downarrow^{\times 1/2}\rightarrow$ | 2.00 | | | | 2.00 |
| O(2) | 1.54 | | $0.14^{\times 2}\downarrow^{\times 1/2}\rightarrow$ | 1.61 | | 0.20 | 0.20 | 2.01 |
| O(3) | $0.63^{\times 2}\downarrow$ $0.50^{\times 2}\downarrow$ | $1.03^{\times 2}\downarrow$ | | 2.16 | | | | 2.16 |
| O(4) | 0.52 | $0.87^{\times 2}\downarrow^{\times 2}\rightarrow$ | | 2.26 | | | | 2.26 |
| OH | | $0.67^{\times 2}\downarrow^{\times 2}\rightarrow$ | | 1.34 | 0.80 | | | 2.14 |
| OW | | | $0.48^{\times 2}\downarrow^{\times 1/2}\rightarrow$ $0.35^{\times 2}\downarrow^{\times 1/2}\rightarrow$ | 0.41 | 0.20 | 0.80 | 0.80 | 2.21 |
| Sum | 6.21 | 5.14 | 2.36 | | 1.00 | 1.00 | 1.00 | |

* Bond-valence parameters are taken from Brese and O'Keeffe (1991) and Burns *et al*. (1997).

crystallizes in space group *Cmcm* and has similar cell parameters ($a$ = 13.952, $b$ = 10.607, $c$ = 7.748 Å) (Surblé *et al*., 2006; Fig. 7*a*). The framework is nearly the same as that of carlosbarbosaite, but in $Cs(UO_2)_2Nb_2(O_{7.5}\square_{0.5})$, 25% of the Nb-bearing polyhedral dimers contain an anion vacancy along their shared O–O edge, and they form corner-sharing pairs of trigonal bipyramids (cf. Gasperin, 1986). The disordered anion vacancies along the Nb–O chains are necessary to maintain overall charge balance for a composition containing a single univalent cation (Gasperin, 1986, 1987; Surblé *et al*., 2006). The U–Nb–O framework architecture may present itself in a more distorted form (space group *Pnma*), in which the tunnels are elliptical in cross-section (Fig. 7*b*) and contain

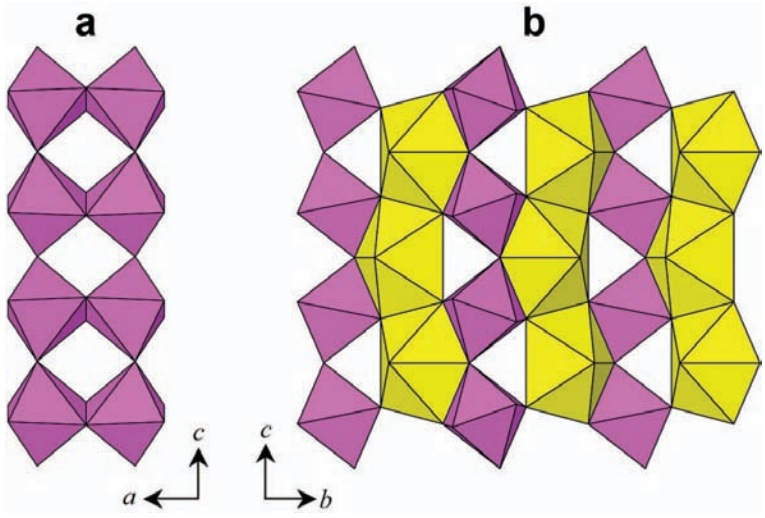


FIG. 4. The structural arrangement of carlosbarbosaite. (*a*) The $Nb_2\varphi_8$ double chain projected onto (010). (*b*) The $UO_5$ chain and $Nb_2\varphi_8$ double chain linkage projected onto (100). The Nb octahedra are pink, U pentagonal bipyramids are yellow.

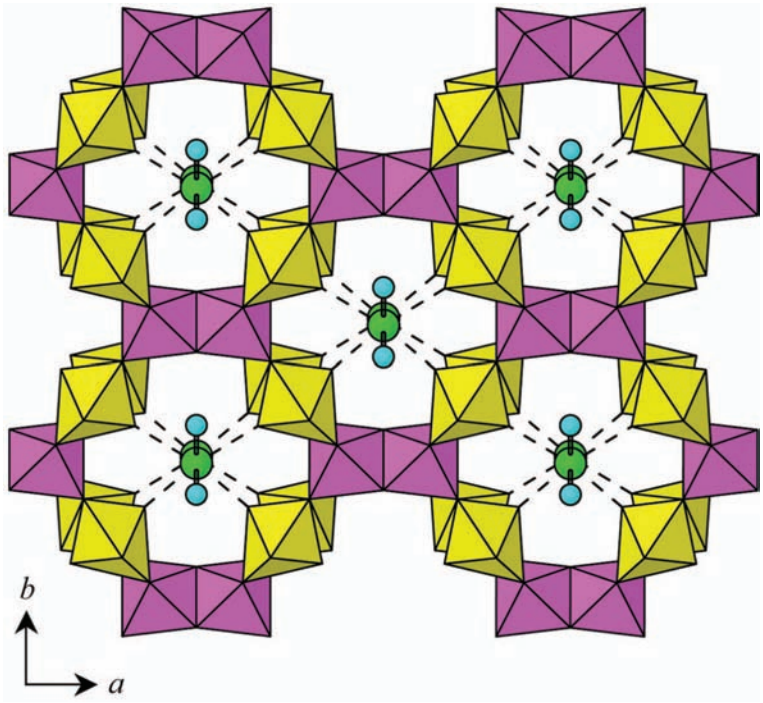


FIG. 5. The U–Nb–φ framework of carlosbarbosaite projected onto (001); $Ca(H_2O)_4$ groups are shown in the tunnels. The Nb octahedra are pink, U pentagonal bipyramids are yellow, Ca atoms are represented by green circles, $H_2O$ groups by blue circles and weak $Ca–O_{uranyl}$ bonds by dashed lines.

either two smaller univalent cations (i.e. $Na^+$ or $K^+$) of the form $(\varphi^+)_2(UO_2)_2Nb_2O_8$ (Surblé *et al*., 2006), or a single larger univalent cation (i.e. $Tl^+$ or $Rb^+$) disordered over the same tunnel site of the form $(\varphi^+)(UO_2)_2Nb_2(O_{7.5}\square_{0.5})$ (Gasperin, 1987; Surblé *et al*., 2006). In the former compounds Nb–O chains contain simple edge-sharing $Nb_2O_{10}$ dimers, and in the latter compounds anion vacancies occur between adjacent Nb atoms (in 25% of cases) resulting in a combination of $Nb_2O_{11}$ corner-sharing pairs of trigonal bipyramids and edge-sharing $Nb_2O_{10}$ dimers. In all of the synthetic U–Nb–O tunnel compounds, the univalent cations are located midway between the uranyl oxygen ions that project from the tunnel walls, *maximizing* the distance between the uranyl oxygen ions and tunnel cations. In carlosbarbosaite, the *Ca* tunnel site is adjacent to the uranyl oxygen ions, *minimizing* the distance between the uranyl oxygen ions and the *Ca* site. The bulky $H_2O$ groups are located midway between the uranyl oxygen ions, and are H-bonded to them (Fig. 6).

## The U–Nb–O framework-tunnel synergy

In synthetic U–Nb–O framework tunnel compounds several crystal-chemical relations are evident: (1) stereochemical variation associated with the distorted $Nb^{5+}$ cation allows octahedral and trigonal bipyramidal geometries, producing a framework that can vary its anion content and overall charge; (2) tunnel cross-sectional shape variation is permitted by flexure across the shared edges of U–O and Nb–O chains; (3) variability in the size and occupancy of univalent tunnel cations that position themselves midway between uranyl oxygen ions bordering the tunnels is coupled to (1) and (2).

The discovery of carlosbarbosaite results in the following additional observations: (1) chemical variation is possible in the anion along the shared edge of the $Nb_2\varphi_{10}$ dimer, namely an (OH) group, that H-bonds to the tunnel constituent; (2) a bulky channel complex, namely a $Ca(H_2O)_4$ group, that carries a $2^+$ charge can be present; (3) a new positioning of the tunnel occupant centred

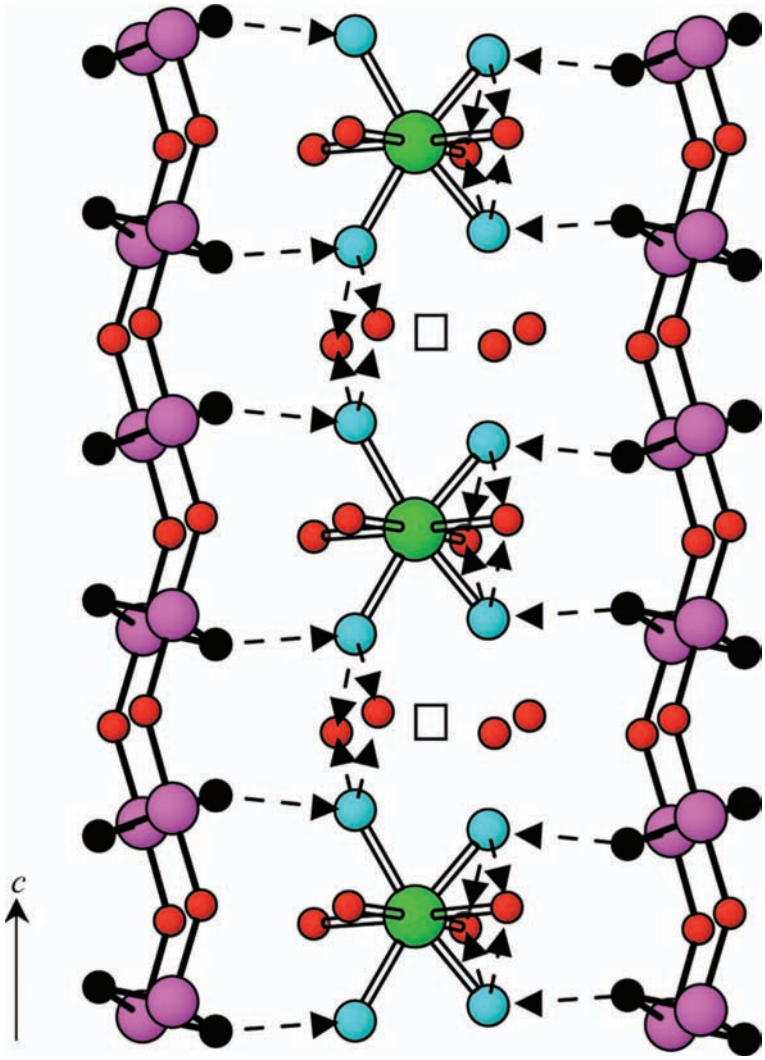


FIG. 6. A cut-away view of the channel in carlosbarbosaite with partial $Nb_2\varphi_8$ double chains at the margins and Ca coordination in the tunnel. The Ca atoms are represented by green circles, $H_2O$ groups by blue circles, (OH) groups by black circles, O atoms by red circles, Nb atoms by pink circles and directed H-bonds by dashed arrows.

adjacent to the uranyl oxygen ions bordering the tunnels is coupled to (1) and (2).

With the structural diversity of U–Nb–O framework tunnel structures to act as a guide, it is tempting to envision further modifications such as protonation of the Nb octahedron, in combination with occupation of the tunnel by a large univalent cation. A more detailed examination of the $Cs(UO_2)_2Nb_2(O_{7.5}\square_{0.5})$ compound of Surblé *et al*. (2006) results in the bond valence analysis given in Table 9 and the O(5) environment shown in Fig. 8*a*. It is immediately apparent that the O(5) anion (along the shared $Nb_2O_{10}$ edge) is very under-bonded (with a bond valence sum of 1.50 vu). The channel Cs, which is 4.17 Å away, offers no significant additional valence contribution, and we are left with the supposition that this highly undersaturated anion is a salient feature of the structure. If we now envision a simple protonation of half of the O(5) anions, to

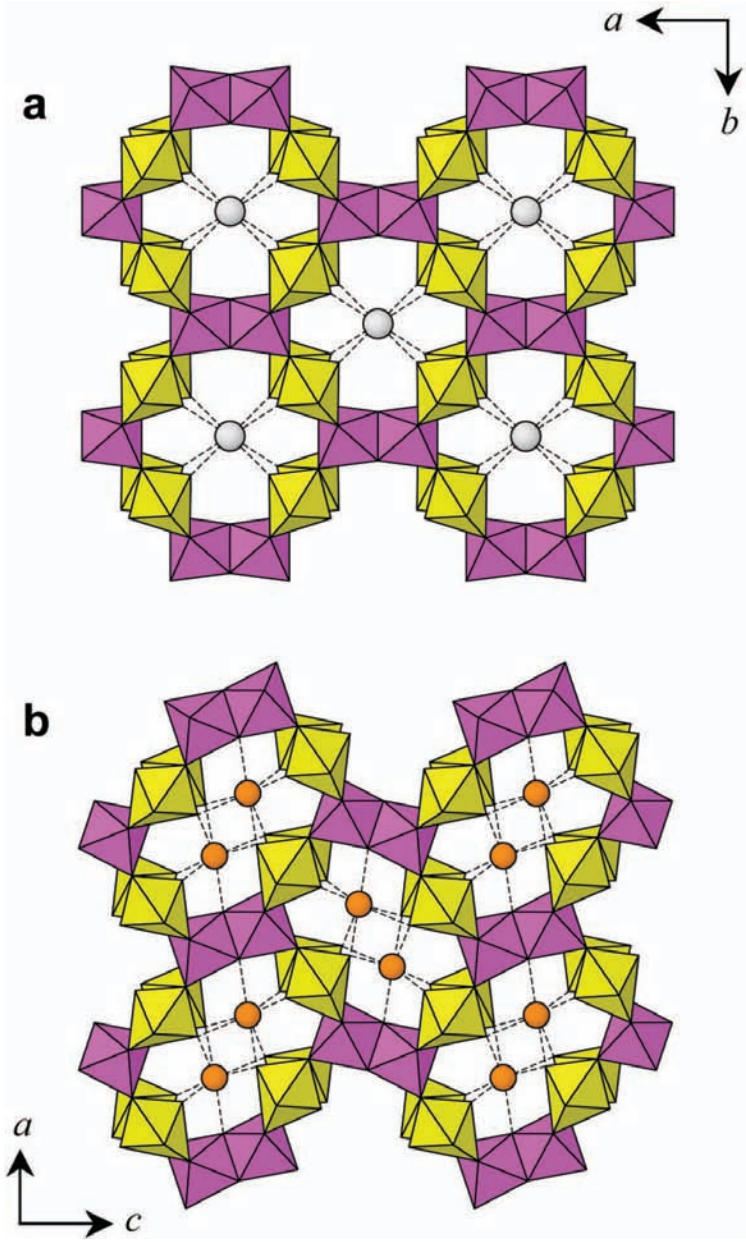


FIG. 7. The U–Nb–O framework of (*a*) $Cs(UO_2)_2Nb_2(O_{7.5}\square_{0.5})$ projected onto (001), and (*b*) $K_2(UO_2)_2Nb_2O_8$ projected onto (010), Surblé *et al*. (2006). The Nb octahedra are pink, U pentagonal bipyramids are yellow, Cs atoms are represented by grey circles and K atoms by orange circles.

form (OH) groups, with the other half of the O(5) anions acting as H-bond acceptors, an equitable bond valence summation at all O(5) anions is easily achieved with minor complimentary Nb–O(5) bond length adjustments (Fig. 8*b*). We note that the average of the two proposed Nb–O(5) distances [(2.10 + 1.95)/2 = 2.025 Å] and their associated average bond valence

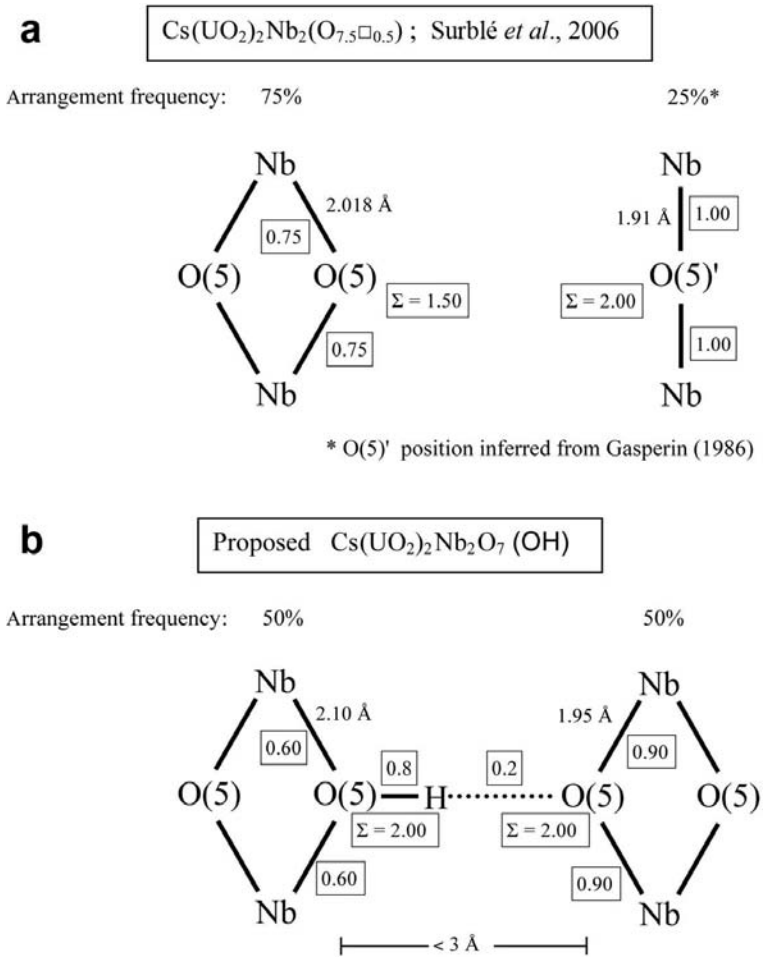


FIG. 8. The local O(5) bonding environments in (*a*) $Cs(UO_2)_2Nb_2(O_{7.5}\square_{0.5})$, Surblé *et al*. (2006), and (*b*) the proposed $Cs(UO_2)_2Nb_2O_7(OH)$. Bond valence values (vu) are shown in boxes.

TABLE 9. Bond-valence analysis for $Cs(UO_2)_2Nb_2(O_{7.5}\square_{0.5})$.*

| | *U* | *Nb* | *Cs* | Sum |
|---|---|---|---|---|
| O(1) | $0.49^{\times 2}\downarrow$ $0.60^{\times 2}\downarrow$ | $0.86^{\times 2}\downarrow$ | | 1.95 |
| O(2) | 0.52 | $0.74^{\times 2}\downarrow^{\times 2}\rightarrow$ | | 2.00 |
| O(3) | 1.66 | | $0.11^{\times 4}\downarrow^{\times 2}\rightarrow$ | 1.88 |
| O(4) | 1.68 | | $0.10^{\times 4}\downarrow^{\times 2}\rightarrow$ | 1.88 |
| O(5) | | $0.75^{\times 2}\downarrow^{\times 2}\rightarrow$ | | 1.50 |
| Sum | 6.04 | 4.70 | 0.84 | |

* Bond-valence parameters are taken from Brese and O'Keeffe (1991) and Burns *et al*. (1997).

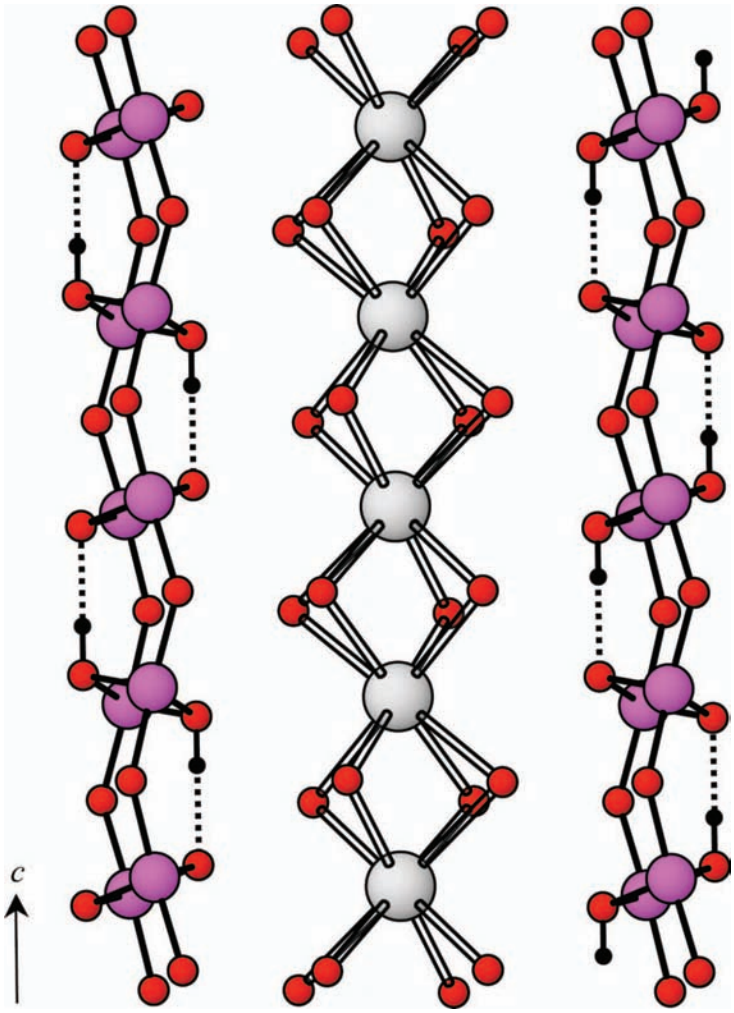


FIG. 9. A cut-away view of the tunnel in the proposed $Cs(UO_2)_2Nb_2O_7(OH)$ compound showing the H-bonding along the tunnel wall between neighbouring O(5) sites. The Nb atoms are indicated by pink circles, O atoms by red circles, H atoms by black circles, Cs atoms by grey circles and H-bonds by dashed lines.

[(0.60 + 0.90)/2 = 0.75 vu] are in good agreement with the observed Nb−O(5) bond length of 2.018 Å and calculated bond valence of 0.75 vu in $Cs(UO_2)_2Nb_2(O_{7.5}\square_{0.5})$ (Surble *et al*., 2006). The proposed H-bonding scheme is shown in Fig. 9, with the H-bonds directed along the walls of the channel. The Cs position is located >4.3 Å from the H position, and its presence in the channel does not present a problem with regard to mutual occupation by H and Cs. The resulting formula is $Cs(UO_2)_2Nb_2O_7(OH)$. The proposed structural arrangement offers an interesting alternative to the unprotonated $Cs(UO_2)_2Nb_2(O_{7.5}\square_{0.5})$ compound proposed by Surblé *et al*. (2006). The latter compound was synthesized in air and allowed to cool slowly to room temperature; it is recommended that structures containing tunnels that are amenable to H-bearing species are analysed by IR or Raman spectroscopy to determine the presence or absence of (OH) and $H_2O$ groups.

## Acknowledgements

We acknowledge FAPESP (Fundação de Amparo à Pesquisa do Estado de São Paulo) for financial

support (Process 2009/09125-5); Frank Hawthorne for the use of his single-crystal X-ray diffractometer; Isaac Jamil Sayeg for the preliminary EDS analysis; Liz Zanchetta D'Agostino for the carlosbarbosaite SEM photos; the members of the Commission on New Minerals Nomenclature and Classification of the International Mineralogical Association (CNMNC - IMA) for their helpful suggestions and comments; and the editors Mark Welch and Pete Williams, the Associate Editor Elena Sokolova, and two anonymous reviewers for their constructive comments.

## References

Abd El-Naby, H.H. (2008) Genesis of secondary uranium minerals associated with jasperoid veins, El Rerdiya area, Eastern Desert, Egypt. *Mineralium Deposita*, **41**, 933–944.

Arcidiácono, E.C. and Bedlivy, D. (1976) Datos preliminares sobre el hallazgo de un nuevo mineral de uranio, en Tanti (Prov. de Cordoba, R. Argentina). *Revista de la Asociación Geológica Argentina*, **31**, 232–234.

Atencio, D., Andrade, M.B., Christy, A.G., Gieré, R., Kartashov, P.M. (2010) The pyrochlore supergroup of minerals: nomenclature. *The Canadian Mineralogist*, **48**, 673–698.

Belakovskiy, D.I., Pautov, L.A., Sokolova, E., Hawthorne, F.C. and Mokhov, A.V. (2006) Holfertite, a new hydroxyl-hydrated uranium titanate from Starvation Canyon, Thomas Range, Utah. *Mineralogical Record*, **37**, 311–317.

Brese, N.E. and O'Keeffe, M. (1991) Bond-valence parameters for solids. *Acta Crystallographica*, **B47**, 192–197.

Burns, P.C., Ewing, R.C. and Hawthorne, F.C. (1997) The crystal chemistry of hexavalent uranium: polyhedral geometries, bond-valence parameters, and polymerization of polyhedra. *The Canadian Mineralogist*, **35**, 1551–1570.

Cassedanne, J.P. and Alves, J.N. (1994) The Jaguaraçu pegmatite, Minas Gerais, Brazil. *Mineralogical Record*, **25**, 165–170.

Edge, R.A. and Taylor, H.F. (1971) Crystal structure of thaumasite, $[Ca_3Si(OH)_6{\cdot}12H_2O](SO_4)(CO_3)$. *Acta Crystallographica*, **B27**, 594–601.

Foord, E.E., Gaines, R.V., Crock, J.G., Simmons, W.B., Jr. and Barbosa, C.P. (1986) Minasgeraisite, a new member of the gadolinite group from Minas Gerais, Brazil. *American Mineralogist*, **71**, 603–607.

Gasperin, M. (1986) $(Cs_{.75}K_{.25})(Nb,Ti)U_2O_{11}$: Un niobotitanouranate alcalin de type structural nouveau. *Acta Crystallographica*, **C42**, 136–138.

Gasperin, M. (1987) Synthese et structure de trois niobouranates d'ions monovalents: $TlNb_2U_2O_{11.5}$, $KNbUO_6$, et $RbNbUO_6$. *Journal of Solid State Chemistry*, **67**, 219–224.

Mandarino, J.A. (1979) The Gladstone–Dale relationship: part III. Some general applications. *The Canadian Mineralogist*, **17**, 71–76.

Mandarino, J.A. (1981) The Gladstone–Dale relationship: part IV. The compatibility concept and its application. *The Canadian Mineralogist*, **19**, 441–450.

Mandarino, J.A. (1989) The Gladstone–Dale compatibility of some new mineral proposals considered by the Commission on New Minerals and Mineral Names, I.M.A. (1983–1987). *European Journal of Mineralogy*, **1**, 123–125.

Moore, P.B., Barbosa, C.P. and Gaines, R.V. (1978) Bahianite, $Sb_3Al_5O_{14}(OH)_2$, a new species. *Mineralogical Magazine* **42**, 179–182.

Nomura, S.F., Atencio, D., Chukanov, N.V., Rastsvetaeva, R.K., Coutinho, J.M.V. and Karipidis, T. (2010) Manganoeudialyte, a new mineral from Poços de Caldas, Minas Gerais, Brazil. *Zapiski RMO (Proceedings of the Russian Mineralogical Society)*, **139**, 35–47.

O'Keeffe, M. and Hyde, B.G. (1981). The role of nonbonded forces in crystals. Pp. 227–254 in: *Structure and Bonding in Crystals* (M. O'Keeffe and A. Navrotsky, editors). Wiley, New York.

Sheldrick, G.M. (1997) *SHELX-97: Program for the solution and refinement of crystal structures*. Siemens Energy and Automation, Madison, Wisconsin, USA

Sheldrick, G.M. (1998) *SADABS User Guide*. University of Göttingen, Göttingen, Germany.

Sokolova, E., Hawthorne, F.C., Belakovskiy, D.I. and Pautov, L.A. (2005) The OD (Order-Disorder) structure of holfertite, $[U^{6+}_{1.75}Ti^{4+}O(OH)][(H_2O)_3(Ca_{0.25}]$, a new mineral from Searle Canyon, Thomas Range, Utah, USA. *The Canadian Mineralogist*, **43**, 1545–1552.

Smith, D.G.W. and Nickel, E.H. (2007) A system for codification for unnamed minerals: report of the Subcommittee for Unnamed Minerals of the IMA Commission on New Minerals, Nomenclature and Classification. *The Canadian Mineralogist*, **45**, 983–1055.

Surblé, S., Obbade, S., Saad, S., Yagoubi, S., Dion, C. and Abraham, F. (2006) The $A_{(1-x)}$ U Nb $O_{(6-x/2)}$ compounds (x = 0, A = Li, Na, Cs and x = 0.5, A = Rb, Cs): from layered to tunneled structure. *Journal of Solid State Chemistry*, **179**, 3238–3251.